

Leukocytes from obese individuals exhibit an impaired SPM signature

AQ:1
 AQ:2
 AQ:3

Cristina López-Vicario,^{*1} Esther Titos,^{*,†} Mary E. Walker,[‡] José Alcaraz-Quiles,^{*} Mireia Casulleras,^{*} Marta Durán-Güell,^{*} Roger Flores-Costa,^{*} Noelia Pérez-Romero,[§] Montserrat Forné,[¶] Jesmond Dalli,[‡] and Joan Clària^{*,†,||,2}

^{*}Biochemistry and Molecular Genetics Service, Hospital Clínic–Institut d’Investigacions Biomèdiques August Pi i Sunyer (IDIBAPS)–University of Barcelona, Centro de Investigación Biomédica en Red de Enfermedades Hepáticas y Digestivas (CIBERehd), Madrid, Spain; [†]Department of Biomedical Sciences, University of Barcelona, Barcelona, Spain; [‡]Lipid Mediator Unit, Biochemical Pharmacology, William Harvey Research Institute, Barts and the London School of Medicine, Queen Mary University of London, London, United Kingdom; [§]Surgery Department and [¶]Gastroenterology Department, Hospital Universitari Mútua Terrassa, Terrassa, Spain; and ^{||}European Foundation for the Study of Chronic Liver Failure (EF Clif), Barcelona, Spain

ABSTRACT: Specialized proresolving mediators (SPMs) biosynthesized from docosahexaenoic acids (DHAs) including resolvins (Rvs), protectins, and maresins are potent endogenous autacoids that actively resolve inflammation, protect organs, and stimulate tissue regeneration. Our hypothesis was that failure of resolution programs may lead to unremitting inflammation in obesity, contributing to the development of metabolic comorbidities in this condition. Obese individuals with persistent low-grade systemic inflammation showed reduced leukocyte production of the DHA-derived monohydroxy fatty acid 17-hydroxy-DHA (HDHA) and unbalanced formation of SPMs (in particular D-series Rvs) accompanied by enhanced production of proinflammatory lipid mediators such as leukotriene B₄. Mechanistic studies attributed this impairment to reduced 15-lipoxygenase (LOX) activity rather than altered DHA cellular uptake. Moreover, leukocytes from obese individuals exhibited decreased 5-LOX levels and reduced 5-LOX Ser271 phosphorylation and distinct intracellular 5-LOX redistribution. However, 15-LOX appears to be the most critical factor for the deficient production of SPMs by obese leukocytes because the formation of D-series Rvs was completely rescued by incubation with the intermediate precursor 17-HDHA. These data provide proof of concept that administration of intermediate precursors of SPM biosynthesis (e.g., 17-HDHA) could be more efficient in overriding impaired formation of these proresolving lipid mediators in conditions characterized by dysfunctional LOX activity, such as obesity.—López-Vicario, C., Titos, E., Walker, M. E., Alcaraz-Quiles, J., Casulleras, M., Durán-Güell, M., Flores-Costa, R., Pérez-Romero, N., Forné, M., Dalli, J., Clària, J. *Leukocytes from obese individuals exhibit an impaired SPM signature.* *FASEB J.* 33, 000–000 (2019). www.fasebj.org

KEY WORDS: specialized proresolving mediator · lipoxygenases · obesity

AQ:4 ABBREVIATIONS: AA, arachidonic acid; BMI, body mass index; COX, cyclooxygenase; CYP, cytochrome P450; DHA, docosahexaenoic acid; DPBS, Dulbecco’s PBS; EPA, eicosapentaenoic acid; FLAP, 5-LOX activating protein; GAPDH, glyceraldehyde-3-phosphate dehydrogenase; HDHA, hydroxy-DHA; HEPE, hydroxy-EPA; HETE, hydroxyeicosatetraenoic acid; LC-MS/MS, liquid chromatography–tandem mass spectrometry; LOX, lipoxygenase; LT, leukotriene; LX, lipoxin; MaR, maresin; MFSD2A, major facilitator superfamily domain-containing protein 2; MIP, macrophage inflammatory protein; NAFLD, nonalcoholic fatty liver disease; PBMC, peripheral blood mononuclear cell; PG, prostaglandin; phospho, phosphorylated; PMN, polymorphonuclear neutrophil; Rv, resolvins; SPM, specialized proresolving mediator; TX, thromboxane

¹ Correspondence: Department of Biochemistry and Molecular Genetics, Hospital Clínic, Villarroel 170, 08036 Barcelona, Spain. E-mail: clopezv@clinic.cat

² Correspondence: Department of Biochemistry and Molecular Genetics, Hospital Clínic, Villarroel 170, 08036 Barcelona, Spain. E-mail: jclaria@clinic.cat

doi: 10.1096/fj.201802587R

This article includes supplemental data. Please visit <http://www.fasebj.org> to obtain this information.

A persistent subclinical state of low-grade inflammation largely dictates the progression of metabolic complications in obese individuals such as insulin resistance, atherosclerosis, type 2 diabetes, and nonalcoholic fatty liver disease (NAFLD) (1, 2). This state of low-grade inflammation associated with obesity involves many components of the classic inflammatory response to pathogens and includes systemic increases in circulating inflammatory cytokines and acute phase proteins (e.g., C-reactive protein), decreases in insulin-sensitizing and anti-inflammatory factors such as adiponectin, and recruitment and subsequent activation of leukocytes into inflamed tissues (3, 4). The nature of obesity-induced inflammation, which is known as meta-inflammation, is unique compared with other inflammatory conditions because it is characterized by tonic low-grade activation of the immune system in the absence of active infection and in response to recurrent episodes of overnutrition (5).

Moreover, unremitting inflammation in obese individuals could also be the consequence of an intrinsic inability to resolve the chronic state of low-grade inflammation (5).

Current evidence indicates that inflammation does not switch off in a passive manner but rather involves a program of unique endogenous mechanisms and mediators that orchestrate active resolution in a timely and effective manner (6, 7). Among these, lipid mediators such as lipoxins (LXs), resolvins (Rvs), protectins, and maresins (MaRs), collectively known as specialized proresolving mediators (SPMs), have attracted the most attention (6, 7). SPMs not only act as “braking signals” of the persistent vicious cycle leading to unremitting inflammation but also mainly as promoters of active resolution of inflammation. Indeed, at the preclinical level, therapeutic administration of SPMs has shown to promote resolution of inflamed adipose tissue and to protect mice against obesity-associated complications such as insulin resistance and NAFLD (8–12). Moreover, recent findings have demonstrated that SPMs play a homeostatic role in the human vasculature (13). However, at present, clear proof that the production of SPMs is impaired in the systemic circulation of obese subjects is still lacking.

The aim of the current study was to advance the concept of impaired resolution in human obesity as a phenomenon dictating the inability to suppress unremitting inflammation in this condition. The current study explores this possibility by comparing the production of SPMs in peripheral leukocytes isolated from individuals with morbid obesity with those isolated from nonobese controls. The results obtained confirm that leukocytes from obese individuals have an unbalanced formation of SPMs with respect to proinflammatory lipid mediators such as leukotriene (LT) B₄ and prostaglandins (PGs). Moreover, the current study provides new insights into the mechanisms underlying impaired SPM formation in obese leukocytes. Finally, the results of this study offer new therapeutic avenues to normalize SPM production in obese individuals through the administration of monohydroxylated precursors of SPM biosynthesis.

MATERIALS AND METHODS

Study participants

Peripheral venous blood samples (10–20 ml) were collected in EDTA tubes from 26 individuals with a body mass index (BMI) [calculated as mass/(height)²] >30 kg/m² (obese group) and 17 individuals with a BMI <30 kg/m² (nonobese group). Demographic and clinical data and drug use were collected from the electronic medical records. All methods were carried out in accordance with the guidelines and regulations dictated by the Ethics Committee of Clinical Investigation of the Hospital Clínic and Hospital Universitari Mútua de Terrassa. Written informed consent was obtained from all the participants.

Isolation of leukocytes, peripheral blood mononuclear cells, and polymorphonuclear neutrophils and cell incubations

Blood samples were centrifuged at 200 g for 10 min, and sedimented cells were incubated with prewarmed ammonium-

chloride-potassium lysis buffer for 5 min at room temperature to remove red blood cells. The samples were then centrifuged at 400 g for 5 min at 21°C, and the supernatants were decanted. The red blood cell lysis procedure was repeated twice for 5 min each, and the resulting pellet was finally washed with Dulbecco's PBS (DPBS) without calcium and magnesium. The isolated leukocytes were enumerated and resuspended in DPBS with calcium and magnesium (DPBS⁺⁺) and incubated at a density of 3 × 10⁶ cells/ml for 30 min at 37°C in a 5% CO₂ atmosphere and then challenged with zymosan A (100 ng/ml) in the presence of either vehicle (0.03% ethanol), eicosapentaenoic acid (EPA) (1 μM), docosahexaenoic acid (DHA) (1 μM), 18-hydroxy-EPA (HEPE) (1 μM), or 17S-hydroxy-DHA (HDHA) (1 μM). After 30 min of incubation, the samples were centrifuged at 1000 g for 5 min, and pellets and supernatants were stored at –80°C for further analysis. Peripheral blood mononuclear cells (PBMCs) and polymorphonuclear neutrophils (PMNs) from obese and non-obese individuals were separated using the Ficoll-Hypaque Plus (GE Healthcare, Waukesha, WI, USA) density gradient with equal volumes and spun at 700 g for 30 min at room temperature. After centrifugation, the Ficoll-Hypaque layers were aspirated, and PBMCs and PMNs were collected on the corresponding layers at densities ranging from 1.024 to 1.077 g/ml and 1.077 to 1.119 g/ml, respectively. Individual PBMC and PMN suspensions were washed twice with DPBS, centrifuged, resuspended in 1 ml of DPBS, and either stored at –80°C for protein analysis or fixed with 4% paraformaldehyde for immunocytochemistry. AQ:5

Major facilitator superfamily domain-containing protein 2 immunocytochemistry

Isolated PMNs and PBMCs from nonobese and obese individuals were deposited on glass slides by cytospin centrifugation (100,000 cells/cover slip) and fixed with fresh 4% paraformaldehyde for 20 min at room temperature followed by incubation with peroxidase blocking solution (S2023; Agilent Technologies, Santa Clara, CA, USA) for 15 min at room temperature and incubated with blocking serum [Vectastin Avidin-Biotin Complex Kit; Vector Laboratories, Burlingame, CA, USA]. The cells were then incubated overnight at 4°C with the primary rabbit anti-major facilitator superfamily domain-containing protein 2 (MFS2A) pAb (ab105399, dilution 1/50; Abcam, Cambridge, United Kingdom) followed by incubation for 30 min at room temperature with a biotinylated anti-rabbit IgG secondary antibody and incubation with avidin-biotin complex for 30 min at room temperature. Color was developed using the diaminobenzidine substrate (Roche, Basel, Switzerland), and the cells were counterstained with hematoxylin, mounted with aqueous solution, and visualized in an Eclipse E600 microscope (Nikon, Tokyo, Japan). AQ:6

Targeted lipid mediator profiling

Plasma and cell incubations were placed in 2 volumes of methanol containing deuterium-labeled d₇-LXA₄, d₅-RvD₂, d₄-PGE₂, d₄-LTB₄, and d₈-5S-hydroxyeicosanoic acid (HETE) (500 pg each), kept at –20°C for a minimum of 45 min to allow protein precipitation, and then centrifuged at 1500 g for 10 min at 4°C. All samples for liquid chromatography–tandem mass spectrometry (LC-MS/MS)-based profiling were extracted using solid-phase extraction columns as in refs. 14 and 15. Briefly, supernatants were subjected to solid-phase extraction, and methyl formate fractions were collected and brought to dryness. The extracts were resuspended in methanol and water (1:1, v/v) for injection on an LC-20AD HPLC equipped with an SIL-20AC autoinjector (Shimadzu, Kyoto, Japan) paired with a QTrap 5500 (Sciex, Framingham, MA, USA). An Agilent Poroshell 120 EC-C18 column

(100 mm × 4.6 mm × 2.7 μm) was kept at 50°C, and mediators were eluted using a mobile phase consisting of methanol-water-acetic acid of 20:80:0.01 (v/v/v) that was ramped to 50:50:0.01 (v/v/v) over 0.5 min and then to 80:20:0.01 (v/v/v) from 2 to 11 min, maintained until 14.5 min, and then rapidly ramped to 98:2:0.01 (v/v/v) for the next 0.1 min. This was subsequently maintained at 98:2:0.01 (v/v/v) for 5.4 min, and the flow rate was maintained at 0.5 ml/min. The QTrap 5500 was operated using a multiple reaction monitoring method (14, 15). Each metabolite was identified using established criteria, including matching retention times to synthetic materials and authentic material and at least 6 diagnostic ions in the tandem mass spectrum (14, 15). Calibration curves were obtained for each lipid mediator using synthetic and authentic standard mixtures at 0.78, 1.56, 3.12, 6.25, 12.5, 25, 50, 100, and 200 pg that gave linear calibration curves with r^2 values of 0.98–0.99.

Assessment of thromboxane B₂ and 6-keto-PGF_{1α}

Plasma levels of thromboxane (TX)-B₂ and 6-keto-PGF_{1α} were measured *via* ELISA (Cayman Chemicals, Ann Arbor, MI, USA), following the manufacturer's recommendations.

Assessment of cytokines and chemokines by Luminex xMap technology

Cytokine and chemokine levels were determined using a multiplex bead-based immunoassay (Human Cytokine/Chemokine Magnetic bead panel Premixed 38 Plex Kit; MilliporeSigma, Burlington, MA, USA) in a Luminex 100 Bioanalyzer (Luminex, Austin, TX, USA). Briefly, 25 μl plasma was added to each well before the addition of 25 μl premixed microbeads. The plate was incubated overnight at 4°C with shaking, then washed and reincubated with 25 μl detection antibody for 1 h. The plate was washed again and incubated with 25 μl streptavidin-phycoerythrin for 30 min. Finally, after 2 washes, the beads were resuspended in 100 μl sheath fluid and analyzed in the Luminex 100 system. The readouts were analyzed with the standard version of Milliplex Analyst software (MilliporeSigma). A 5-parameter logistic regression model was used to create standard curves (picograms per milliliter) and to calculate the concentration of each sample. Among the 38 cytokines and chemokines, only 15 were detected in plasma of obese and nonobese individuals: TNF-α, monocyte chemoattractant protein 1, IL-1β, -6, -10, -17A, macrophage inflammatory protein (MIP) 1α, MIP-1β, C-X-C motif chemokine 10, IFN-γ, IL-4, granulocyte CSF, granulocyte M-CSF, IL-8, and IL-1RA.

AQ:7

Analysis of gene expression by TaqMan low-density arrays

Isolation of total RNA from human leukocytes was performed using Trizol reagent. RNA concentration was assessed in a NanoDrop-1000 spectrophotometer (Thermo Fisher Scientific, Waltham, MA, USA), and its integrity was tested with an RNA 6000 Nano Assay in a Bioanalyzer 2100 (Agilent Technologies). cDNA synthesis from 1 μg of total RNA was performed using the High-Capacity cDNA Archive Kit (Thermo Fisher Scientific) and loaded on customized TaqMan low-density array microfluidic cards (Thermo Fisher Scientific). Probes and primers for arachidonate 5-lipoxygenase (LOX; Hs00167536_m1), arachidonate 15-LOX A (Hs00993765_g1), arachidonate 15-LOX B (Hs00153988_m1), GPR18 (Hs01921463_s1), GPR32 (Hs01102536_s1), formyl peptide receptor 2 (Hs02759175_s1), chemerin receptor 23 (Hs01081979_s1), housekeeping (β-actin, Hs01060665_g1), and 1 positive control for the reaction (18S, Hs99999901_s1) were

AQ:8

preloaded in the 384 wells of each TaqMan low-density array card. Real-time RT-PCR amplifications were carried out in an ABI Prism 7900HT Sequence Detection System and the results were analyzed with the Sequence Detector Software v.2.1 (Thermo Fisher Scientific). Relative quantification of gene expression was performed using the comparative C_t method. The amount of target gene, normalized to β-actin and relative to a calibrator, was determined by the arithmetic equation $2^{-\Delta\Delta C_t}$ described in the comparative C_t method (https://assets.thermofisher.com/TFS-Assets/LSG/manuals/cms_040980.pdf).

Analysis of protein expression by Western blot

Total protein from leukocytes was extracted with lysis buffer containing 50 mM HEPES, 20 mM β-glycerophosphate, 2 mM EDTA, 1% Igepal, 10% (vol/vol) glycerol, 1 mM MgCl₂, 1 mM CaCl₂, and 150 mM NaCl supplemented with protease (Complete Mini; Roche) and phosphatase (PhosStop; Roche) inhibitors. Homogenates were incubated on ice for 15 min and centrifuged at 1000 g for 5 min at 4°C. Total protein (50 μg) from supernatants was placed in SDS-containing Laemmli sample buffer, heated for 5 min at 95°C, and separated by 10% (vol/vol) SDS-PAGE for 90 min at 120 V. Transfer onto PVDF membranes was performed using the iBlot Dry Blotting System (Thermo Fisher Scientific) at 20 V for 7 min, and the efficiency of the transfer was visualized by Ponceau S staining. The membranes were then soaked for 1 h at room temperature in 0.1% T-TBS and 5% (wt/vol) nonfat dry milk. Blots were washed 3 times for 5 min each with 0.1% T-TBS and subsequently incubated overnight at 4°C with primary rabbit anti-human 5-LOX (3289, dilution 1/1000; Cell Signaling Technology, Danvers, MA, USA), phosphorylated (phospho)-Ser271-5-LOX (ab59395, dilution 1/500; Abcam), 5-LOX activating protein (FLAP, ab124714, dilution 1/1000; Abcam), 15-LOX-1 (ab119774, dilution 1/500; Abcam), phospho-p44/42 MAPK (phospho-Erk1/2, 9101, dilution 1/1000; Cell Signaling Technology), p44/42 MAPK (Erk1/2, 4696, dilution 1/2000; Cell Signaling Technology), and MFSD2A (ab105399, dilution 1/500; Abcam) antibodies in 0.1% T-TBS containing 5% bovine serum albumin. Thereafter, the blots were washed 3 times for 5 min each with 0.1% T-TBS and incubated for 1 h at room temperature with a horseradish peroxidase-linked donkey anti-rabbit antibody (1:2000) in 0.1% T-TBS containing 5% nonfat dry milk, and the bands were visualized using the EZ-ECL chemiluminescence detection kit (Biological Industries, Cromwell, CT, USA). To assess housekeeping protein expression, the membranes were stripped at 50°C for 20 min in 100 mM β-mercaptoethanol, 2% (vol/vol) SDS, and 62.5 mM Tris-HCl (pH 6.8) and reblotted overnight at 4°C with primary glyceraldehyde-3-phosphate dehydrogenase (GAPDH) (ab9485, dilution 1/2000; Abcam).

AQ:9

AQ:10

Confocal microscopy

Isolated PMNs and PBMCs from nonobese and obese individuals were plated (200,000/well) on 0.01% poly-L-lysine-precoated 8-well chamber slides (Nunc, Lab-Tek; Thermo Fisher Scientific) and cultured overnight with Roswell Park Memorial Institute 1640 medium containing penicillin (100 U/ml), streptomycin (100 U/ml), L-glutamine (4 mM), and 10% fetal bovine serum in a humidified 5% CO₂ incubator at 37°C. The cells were fixed with fresh 4% paraformaldehyde for 40 min at room temperature followed by permeabilization with 0.1% Triton X-100 for 15 min at room temperature. They were then washed, blocked with 1% bovine serum albumin for 1 h at room temperature, and incubated in a humidified chamber with anti-5-LOX antibody (ab169755, dilution 1/100; Abcam) for 2 h at room temperature followed by goat anti-rabbit IgG-conjugated Alexa Fluor 488 (Thermo Fisher Scientific) for 30 min at room temperature and

AQ:11

counterstained with fluorescently-labeled phalloidin (P1951, dilution 1/1000; MilliporeSigma) and Hoechst (H3570, dilution 1/2000; Molecular Probes, Eugene, OR, USA) for 20 min at room temperature. Coverslips were then mounted on glass slides with ProLong Gold antifade reagent (Thermo Fisher Scientific) and the fluorescent signal was visualized with a confocal laser-scanning microscope (Zeiss LSM 880; Carl Zeiss, Oberkochen, Germany) at a magnification of $\times 630$. ImageJ software (McMaster Biophotonics; National Institutes of Health, Bethesda, MD, USA) was used for image acquisition.

Intracellular calcium mobilization assay

Leukocytes from nonobese and obese individuals were seeded (200,000/well) in a black wall and clear bottom 96-well plate (Costar; Corning, Corning, NY, USA). The cells were incubated with 100 μ l fura-2 for 1 h at 37°C according to the Fura-2 No Wash Calcium Assay Kit (Abcam) instructions, and N-formylmethionyl-leucyl-phenylalanine (100 nM) or zymosan A (100 ng/ml) were added to induce GPCR agonist-mediated intracellular calcium release. Fluorescence intensities were monitored at excitations of 340 and 380 nm and at an emission of 510 nm.

Statistical analysis

Statistical analysis of the results was performed by ANOVA (1-way or 2-way ANOVA) or the unpaired Student's *t* test. Results are expressed as mean \pm SEM and differences considered significant at $P < 0.05$.

RESULTS

The demographic and clinical characteristics of the patients included in the study are shown in Supplemental Table S1. As compared with nonobese individuals ($n = 17$), the obese group ($n = 26$) had an increased BMI and fasting serum glucose and triglycerides levels and a higher white blood cell count at the expense of a higher neutrophil count, with no changes in serum cholesterol, γ -glutamyl transpeptidase, and alanine and aspartate aminotransferase concentrations. There were no significant differences in age between the study groups (Supplemental Table S1). Multianalyte profiling of circulating cytokines and chemokines revealed that obese individuals had increased plasma levels of monocyte chemoattractant protein 1, IL-6, IL-17A, MIP-1 β , C-X-C motif chemokine 10, IFN- γ , and IL-1RA as compared with nonobese subjects, indicating a higher systemic inflammatory tone in obesity (Supplemental Table S2). The LC-MS/MS profiling of the essential polyunsaturated fatty acids and the bioactive lipid mediators derived from these fatty acids (see a schematic diagram in Fig. 1A) revealed similar plasma levels of arachidonic acid (AA), EPA, and DHA (Fig. 1B) and a similar AA:EPA+DHA abundance ratio (Fig. 1C) in obese and nonobese individuals. The most abundant lipid mediators in the circulation, which in addition were significantly decreased in plasma of obese individuals, were TXB₂ (the inactive stable metabolite of TXA₂) (Fig. 1D) and 12-HETE (Fig. 1E) derived from AA *via* cyclooxygenase (COX) and 12-LOX pathways, respectively. Of interest, no

changes in the ratio between the stable PGI₂ metabolite 6-keto-PGF_{1 α} and TXB₂ were observed when both eicosanoids were measured by ELISA, despite the fact that both lipid mediators were significantly decreased in the obese group (Supplemental Fig. S1). Other lipid mediators that were significantly reduced in obese individuals were the monohydroxylated fatty acids 14-HDHA and 17-HDHA derived from DHA and 15-HETE derived from AA (Fig. 1E). In addition, the cytochrome P450 (CYP) products 20-HETE and 18-HEPE, derived from AA and EPA, respectively, were also significantly reduced (Fig. 1F). Finally, we assessed the plasma levels of SPM in obese individuals and compared them with those in nonobese controls. LC-MS/MS analysis for these lipid mediators was performed according to published criteria that include matching retention times and at least 6 characteristic and diagnostic ions for each, as illustrated with the chromatographic peak and the spectrum obtained for RvD5 (Fig. 1G). As shown in Fig. 1H, the formation of 15-LXA₄, an AA-derived SPM generated through the interaction of 15-LOX with 5-LOX, was significantly reduced in plasma of obese individuals. The plasma levels of RvD2 and RvD4 were also lower in obese individuals, although changes did not reach statistical significance (Fig. 1H). Taken together, these results indicate that in the context of low-grade systemic inflammation, obese individuals exhibit an impaired conversion of polyunsaturated fatty acids to downstream products.

Because bioactive lipid mediators in the circulation are mostly produced by cells of the immune system, we next characterized the LC-MS/MS profile of lipid mediators endogenously produced by circulating leukocytes isolated from obese and nonobese individuals. Leukocytes from obese individuals presented a significantly lower content of the polyunsaturated fatty acid DHA (Fig. 2A), although the AA:EPA+DHA ratio was similar in both groups (Fig. 2B). Moreover, the profile of lipid mediators in leukocytes resembled that seen in plasma, with TXB₂ and 12-HETE followed by 15-HETE, 17-HDHA, 18-HEPE, LTB₄, and 20-HETE being the most abundant (Fig. 2C–E). However, levels of lipid mediators were different depending on whether the leukocytes were isolated from obese or non-obese individuals. In particular, leukocytes from obese subjects showed a 4-fold increase in LTB₄ and 20-HETE (Fig. 2D, E) in parallel with impaired capacity to generate monohydroxylated DHA- and EPA-derived products (*i.e.*, 17-HDHA and 18-HEPE) (Fig. 2D, E). Furthermore, a full array of DHA-derived SPM produced *via* 12-LOX (*i.e.*, MaR1 and MaR2) and 15-LOX (*i.e.*, protectin D1) pathways (Fig. 2D) and *via* 15-LOX and 5-LOX interaction (*i.e.*, RvD4, 5, 2, 1, 6, and 3; in order of abundance) (Fig. 2F) were detected in leukocytes from obese and nonobese subjects. Other SPMs, such as Rvs of the E series (*i.e.*, RvE1, -2, and -3) (Fig. 2E), and LXA₄ and LXB₄ (Fig. 2F) generated from EPA and AA, respectively, were also identified. Pie charts depicting the distribution of lipids identified in leukocytes from obese and nonobese individuals are shown in Fig. 2G. Importantly, leukocytes from obese individuals showed a significantly reduced ratio of DHA-derived SPM production with respect to the levels of classic inflammatory lipid mediators such as LTB₄ and

AQ:12

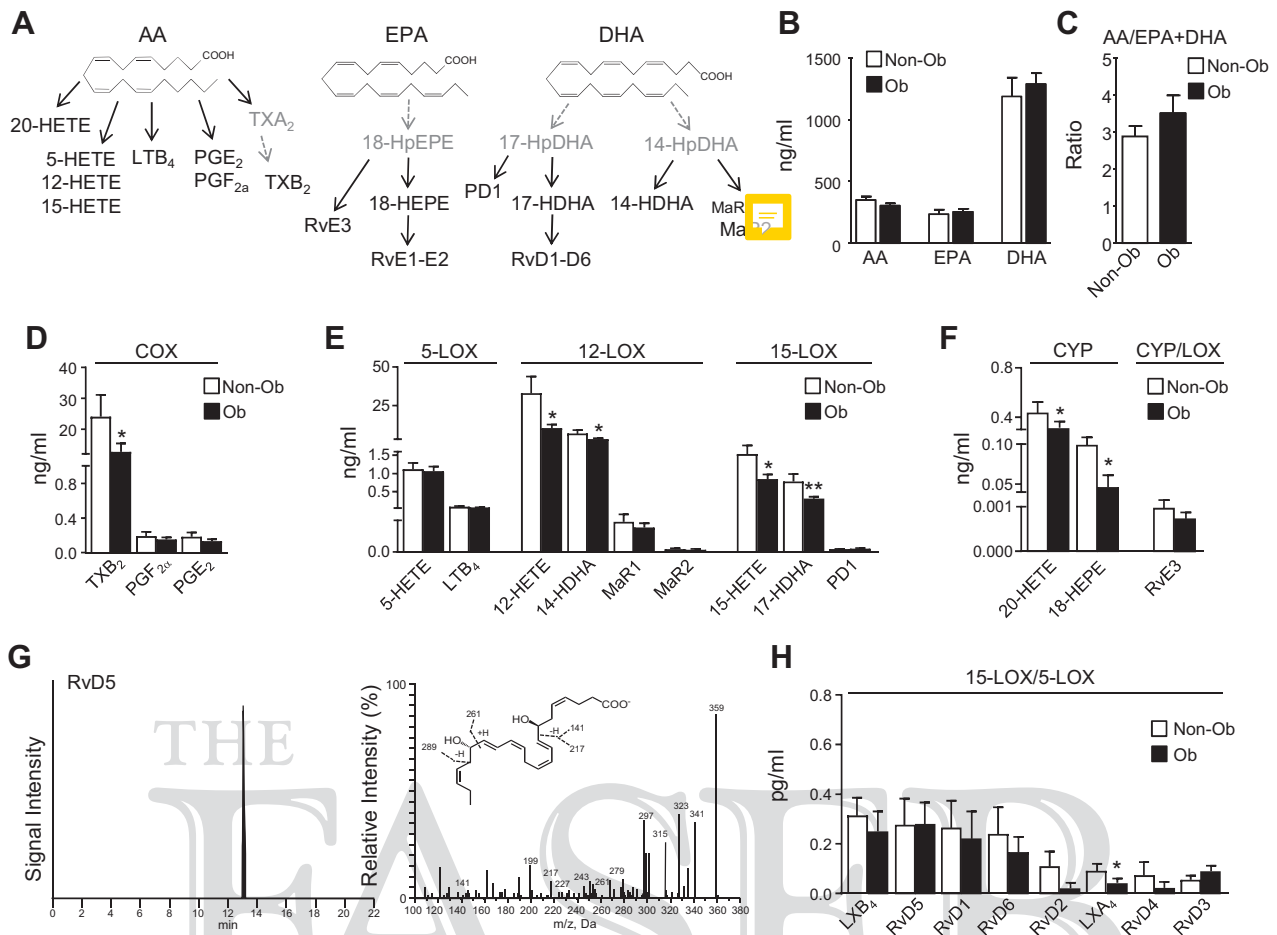


Figure 1. A) Schematic diagram of the biosynthesis of lipid mediators derived from AA, EPA, and DHA. B) Plasma levels of AA, EPA, and DHA in nonobese ($n = 10$) and obese ($n = 20$) subjects as analyzed by LC-MS/MS. C) Plasma AA:(EPA+DHA) ratio in obese and nonobese subjects. D) Plasma levels of COX products derived from AA. E) Plasma levels of 5-, 12-, and 15-LOX products derived from AA and DHA. PD1, protectin D1. F) Plasma levels of CYP and CYP and LOX products from AA and EPA. G) Representative chromatogram and mass spectrum used in the identification of RvD5 by LC-MS/MS-based metabololipidomics. H) Plasma levels of 15-LOX and 5-LOX products from AA and DHA. Non-Ob, nonobese; Ob, obese. Results are expressed as means \pm SEM. * $P < 0.05$, ** $P < 0.01$ vs. Non-Ob group.

PGs (Fig. 3A), a finding that was not as evident in the production of EPA-derived SPMs. Figure 3B provides a detailed distribution of the SPM fractions in these cells from both groups of study.

To investigate the mechanisms responsible for the unbalanced formation of DHA-derived SPMs in leukocytes from obese individuals, we next explored the critical steps involved in the biosynthesis of these proresolving mediators in circulating leukocytes. First, we addressed the cellular DHA uptake through the membrane transporter MFSD2A (16). As shown in Fig. 4A, immunocytochemistry analysis showed that the MFSD2A protein is constitutively expressed in both human PMNs and PBMcs. Of note, the levels of MFSD2A protein expression were significantly reduced in PMNs and PBMcs from obese individuals as compared with those from nonobese controls (Fig. 4B). Because after being taken up by activated leukocytes, DHA is converted into 17-HDHA by 15-LOX, we next assessed the expression of this enzyme in leukocytes from obese individuals. As shown in Fig. 4C, mRNA expression for 15-LOX-1 and 15-LOX-2 (the 2 15-LOX

isoenzymes) were not suppressed but rather increased in leukocytes from obese individuals. Moreover, similar protein levels of 15-LOX-1 were observed in PMNs and PBMcs (Fig. 4D). To determine the relative contribution of each of these 2 mechanisms to the impaired formation of DHA-derived SPMs in obesity, we incubated leukocytes from obese and nonobese individuals with DHA and measured the levels of 17-HDHA produced by these cells. As compared with nonobese leukocytes, obese leukocytes released lower quantities of 17-HDHA from exogenous DHA, indicating either reduced uptake of the fatty acid or reduced 15-LOX activity in these cells (Fig. 4E). However, the levels of other monohydroxy fatty acids derived enzymatically (14-HDHA by 12-LOX) and nonenzymatically (13-HDHA, 7-HDHA, and 4-HDHA) from DHA were not significantly decreased (Fig. 4E). The finding that only 17-HDHA biosynthesis is dependent on 15-LOX together with the observation that endogenous production of other monohydroxy fatty acids was either not different or even increased in obese leukocytes (Fig. 4F) supports the hypothesis of an alteration of 15-LOX activity,

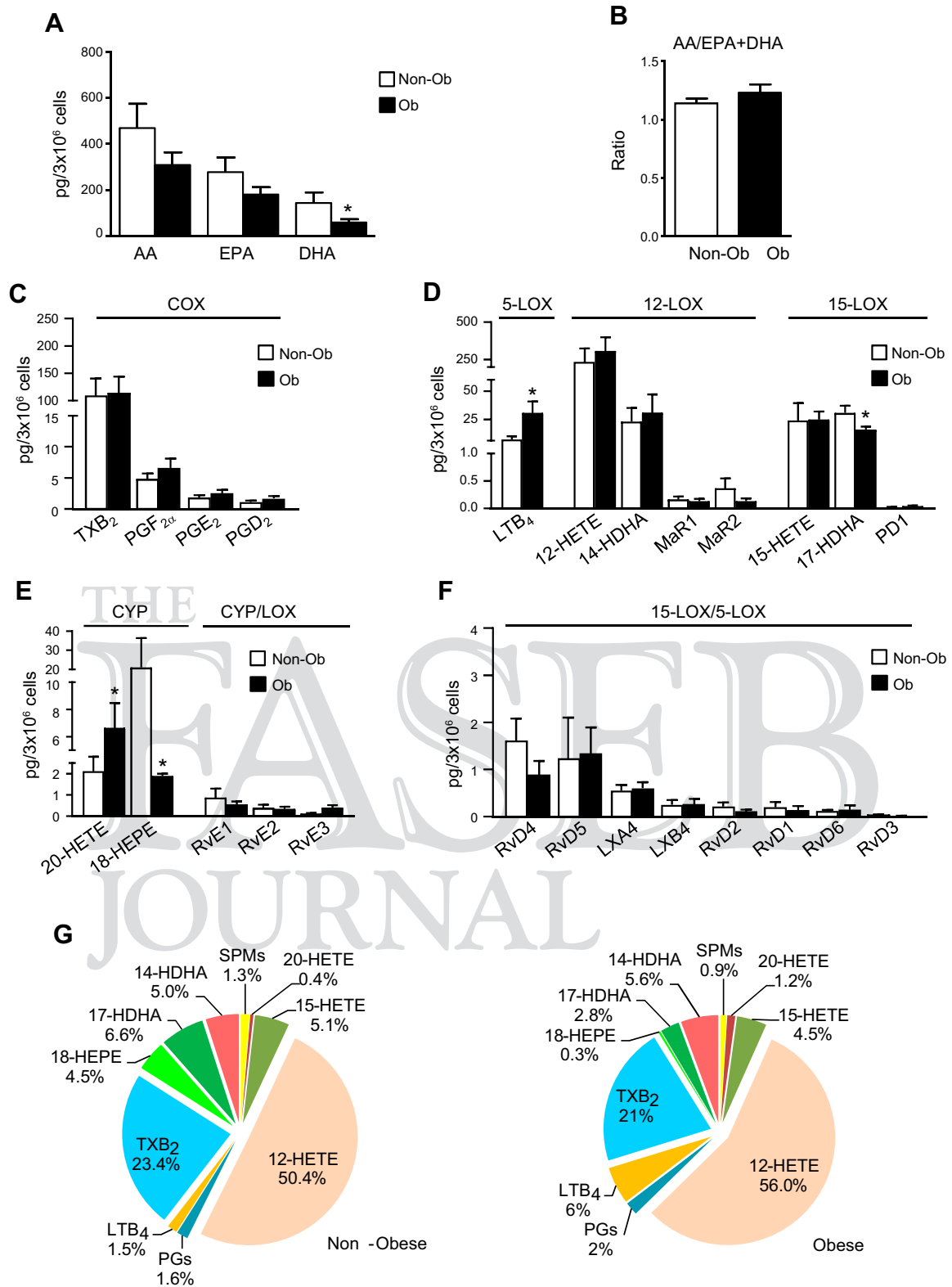


Figure 2. A) Levels of polyunsaturated fatty acids (AA, EPA, and DHA) in isolated leukocytes from nonobese ($n = 5$) and obese ($n = 6$) subjects as analyzed by LC-MS/MS. B) AA:(EPA+DHA) ratio in obese and nonobese individuals. C) Levels of COX products derived from AA. D) Levels of 5-, 12-, and 15-LOX products derived from AA and DHA. E) Levels of CYP and CYP and LOX products from AA and EPA. F) Levels of 15-LOX and 5-LOX products from AA and DHA. G) Pie charts of lipid distribution in leukocytes from obese and nonobese individuals. Non-Ob, nonobese; Ob, obese. Results are expressed as means \pm SEM. * $P < 0.05$ vs. nonobese group.

COLOR

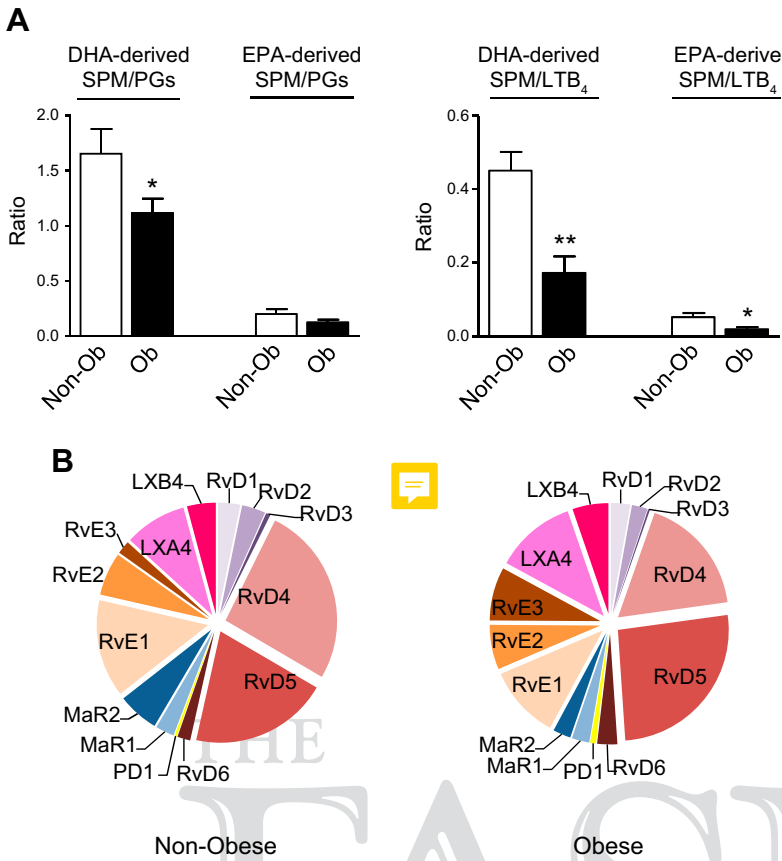


Figure 3. A) DHA- and EPA-derived SPM:LTB₄ (including all LTB₄ metabolome) and DHA- and EPA-derived SPM:PG ratios in leukocytes isolated from nonobese ($n = 5$) and obese ($n = 6$) individuals. B) Pie charts of detailed SPM distribution in leukocytes from obese and non-obese individuals. Non-Ob, nonobese; Ob, obese. Results are expressed as means \pm SEM. * $P < 0.05$, ** $P < 0.01$ vs. nonobese group.

outweighing the importance of the membrane transporter MFSD2A.

Because 17-HDHA is subsequently converted into Rvs of the D series by 5-LOX, we next assessed the expression of this enzyme in leukocytes from obese individuals. As compared with nonobese controls, obese leukocytes showed not only reduced 5-LOX and FLAP protein expression but also decreased phosphorylation of the Ser271 of the 5-LOX enzyme (Fig. 5A). These findings not only indicate a lower amount of 5-LOX enzyme in obese cells but also suggest a distinct localization and redistribution of this enzyme in leukocytes from obese individuals (17–19). Indeed, confocal microscopy imaging revealed that in contrast to nonobese individuals, in whom the 5-LOX signal is abundant and preferentially cytoplasmic, the 5-LOX signal in obese subjects is less intense and more diffusively distributed (Fig. 5B). Figure 5B shows results in PMNs, but similar findings were observed in PBMCs from obese individuals (Supplemental Fig. S2). No changes were seen in Erk1/2 phosphorylation, the upstream kinases that phosphorylate the Ser663 residue in the 5-LOX enzyme (20) (Fig. 5C), and in intracellular calcium mobilization (Fig. 5D), which is a critical factor for the activation of the enzymatic machinery necessary for the biosynthesis of bioactive lipid mediators. Taken together, these findings point to the fact that SPM biosynthesis in leukocytes from obese individuals could also be compromised by poor and unusual intracellular 5-LOX distribution.

We finally monitored the levels of Rvs of the D series in leukocytes incubated with either the parent fatty acid (*i.e.*,

DHA) or the intermediate monohydroxy fatty acid (*i.e.*, 17-HDHA). To assist in understanding these experiments, a simplified scheme of the biosynthesis of D-series Rvs is provided in Fig. 6A. As expected, both DHA and 17-HDHA induced the formation of Rvs of the D series (RvD1, -2, -3, -4, -5, and -6) by leukocytes from healthy donors, with the conversion being more efficient for 17-HDHA than for its parent compound DHA (Fig. 6B). Similarly, the conversion to D-series Rvs was also more efficient for 17-HDHA than for DHA in leukocytes from obese individuals (Fig. 6C). Importantly, when leukocytes from obese individuals were incubated with equimolar concentrations of 17-HDHA, a similar, if not higher, production of D-series Rvs (especially of RvD5) compared with leukocytes from nonobese controls was observed (Fig. 6C). Interestingly, 17-HDHA, but not DHA, significantly reduced LTB₄ release and leukocyte 5-LOX expression (Supplemental Fig. S3A, B). No changes in PG production were seen in these incubations (Supplemental Fig. S3C). It is of major interest that the ratios between D-series Rvs with respect to PGs and LTB₄ were normalized in leukocytes from obese subjects when these cells were incubated with 17-HDHA (Fig. 6D). Similar findings were observed with respect to the formation of Rvs of the E series, when leukocytes were incubated with the 18-HEPE intermediate or its parent compound EPA, in which 18-HEPE was a more efficient substrate for conversion into RvE1, -2, and -3 and normalized the conversion ratio into Rvs of the E series (Supplemental Fig. S4). Notably, 18-HEPE showed a remarkable activity in reversing the up-regulation of

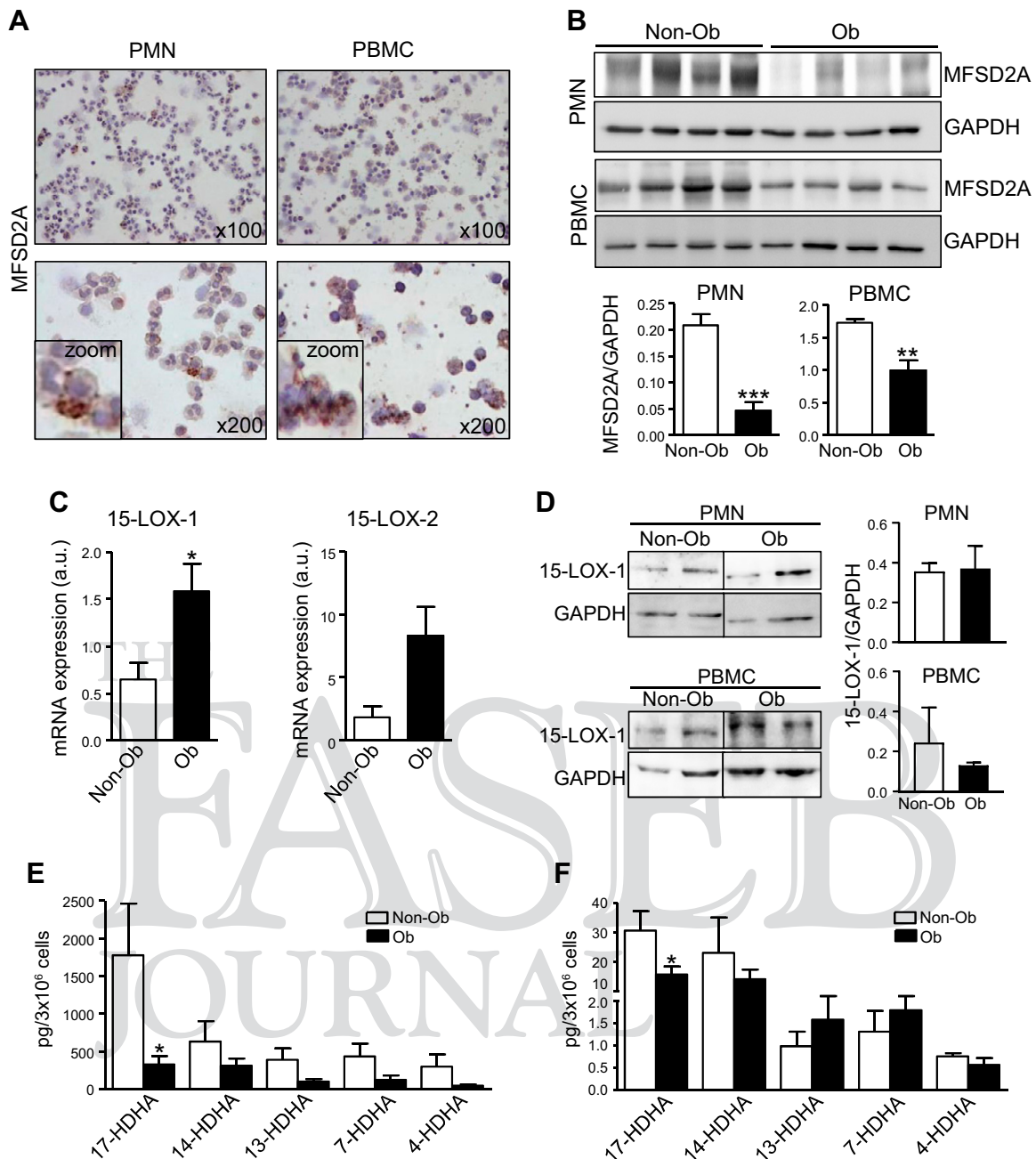


Figure 4. A) Representative immunocytochemistry images of MFSD2A transporter protein staining in PMNs and PBMCs from nonobese ($n = 16$) and obese ($n = 16$) individuals. Original magnification, $\times 100$ (upper panel); original magnification, $\times 200$ (bottom panel). Zoomed images are included in insets. B) Representative immunoblots of MFSD2A and GAPDH assessed by Western blot in PMNs and PBMCs isolated from nonobese ($n = 16$) and obese subjects ($n = 16$). The densitometric analyses of MFSD2A signal normalized to GAPDH are shown at the bottom. C) Gene expression of 15-LOX-1 and 15-LOX-2 enzymes in leukocytes from nonobese and obese individuals. D) Representative immunoblots of 15-LOX-1 and GAPDH assessed by Western blot in PMNs and PBMCs isolated from nonobese ($n = 16$) and obese subjects ($n = 16$). The densitometric analyses of 15-LOX-1 signal normalized to GAPDH are shown at the right. E, F) Production of DHA-derived monohydroxy fatty acids from exogenous (E) and endogenous (F) sources in leukocytes from nonobese ($n = 5$) and obese ($n = 6$) subjects. Non-Ob, nonobese; Ob, obese. Results are means \pm SEM from 3 independent experiments assayed in quadruplicate.

chemerin receptor 23, GPR18, GPR32, and formyl peptide receptor 2 in leukocytes from obese individuals (Supplemental Fig. S5), a finding that can be interpreted as a return to homeostasis of the expression of most of the SPM receptors.

DISCUSSION

Obesity is associated with a generalized state of low-grade inflammation, which is a major risk factor for developing comorbidities within the context of the metabolic syndrome (21). Indeed, obese individuals have an enhanced risk of developing type 2 diabetes, hypertension, and

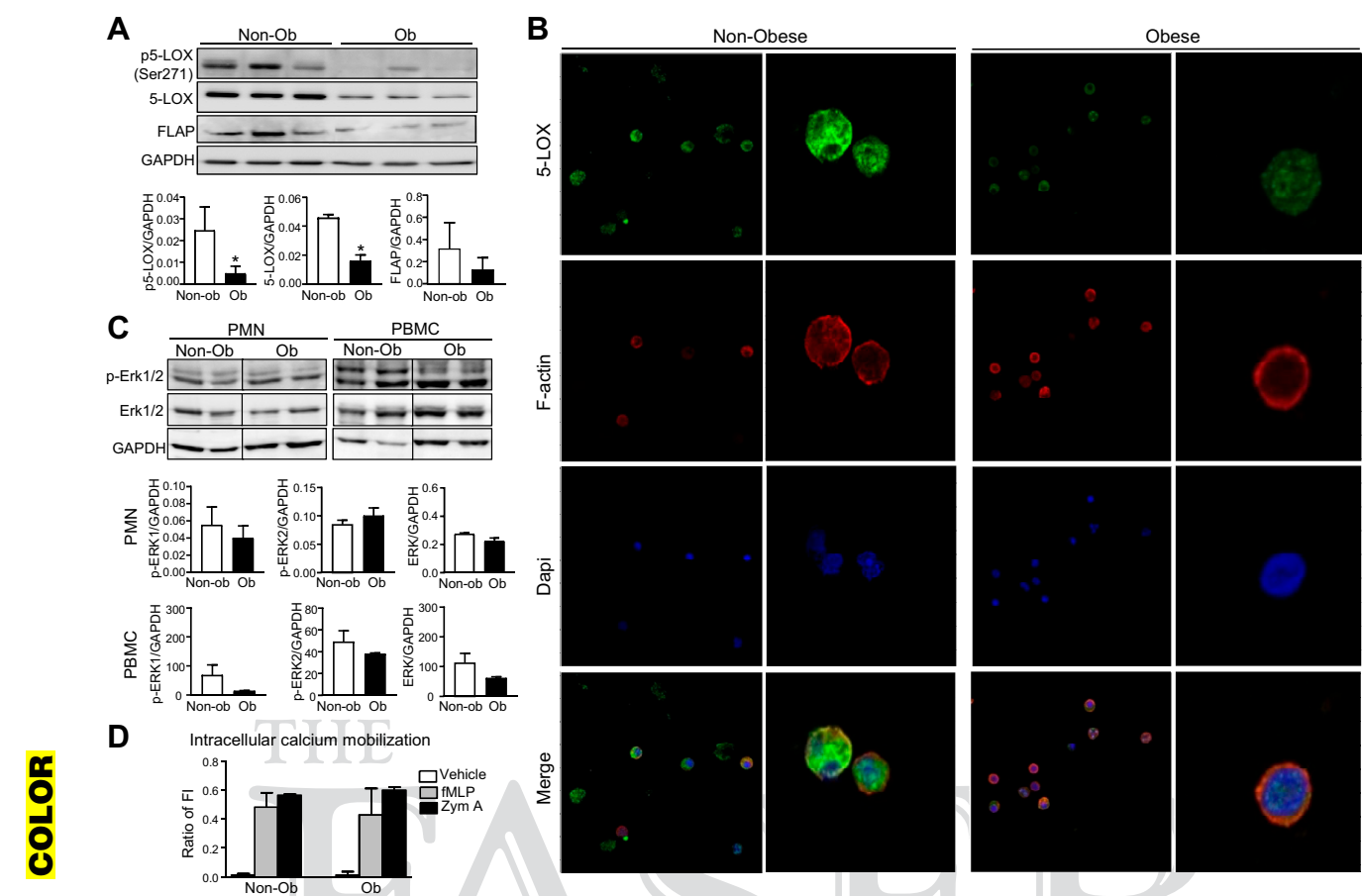
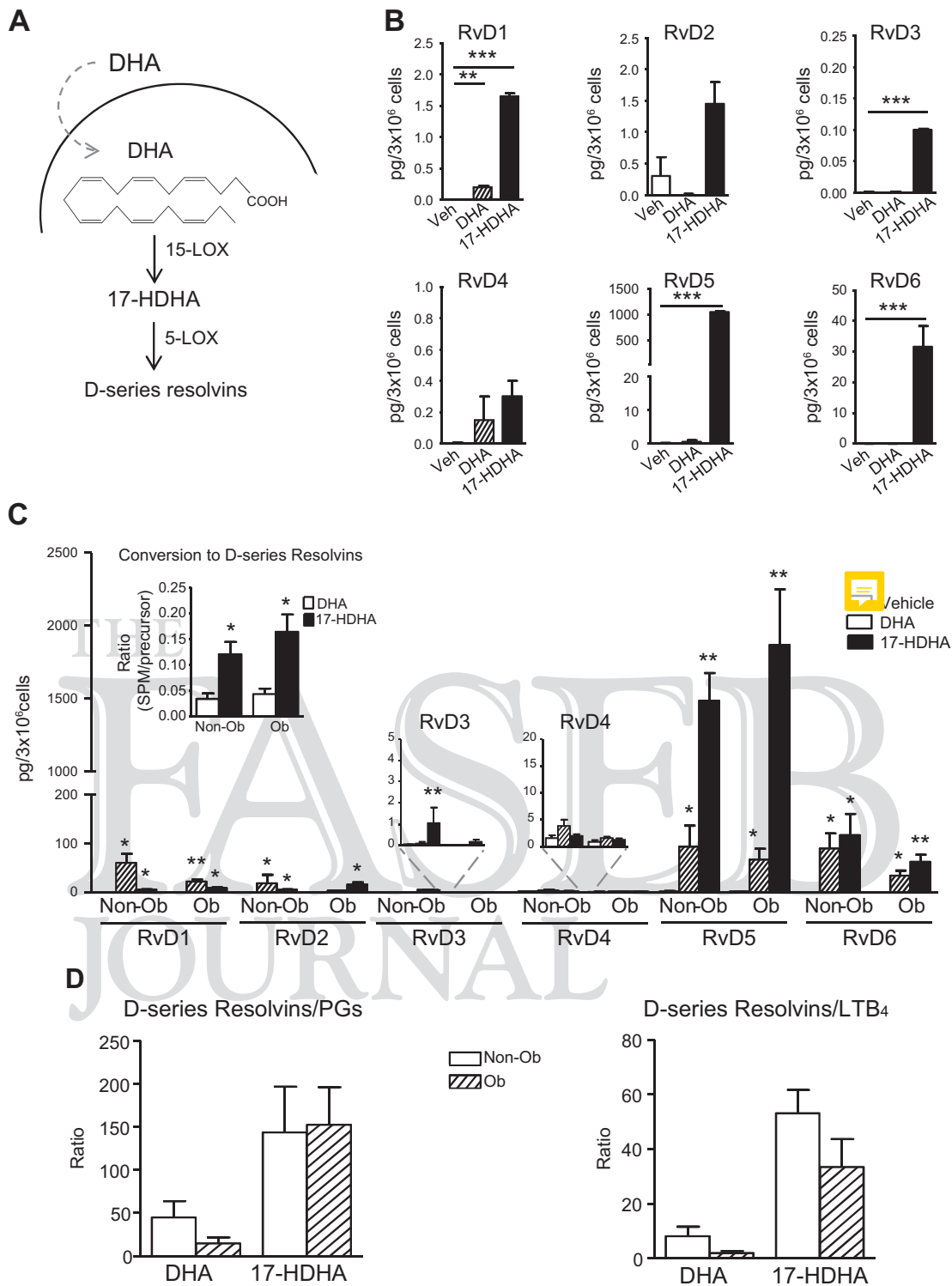


Figure 5. A) Protein expression of phospho-5-LOX (Ser271), total 5-LOX, FLAP, and GAPDH in PMNs from nonobese ($n = 16$) and obese ($n = 16$) subjects assessed by Western blot analysis. The densitometric analyses of phospho-5-LOX, total 5-LOX, and FLAP signals normalized to GAPDH are shown at the bottom. B) Representative confocal laser scanning microscopy images of labeled 5-LOX (green), F-actin (phalloidin, red), and nuclei (DAPI, blue) in PMNs of nonobese ($n = 4$) and obese ($n = 4$) individuals at original magnification, $\times 630$. Merged images are shown in the bottom panel. Representative zoomed images at 3.0 times are also given (middle). C) Representative immunoblots of phospho-Erk1/2 and total Erk1/2 protein expression from nonobese ($n = 16$) and obese subjects ($n = 16$). The densitometric analyses of phospho-Erk1/2 and total Erk1/2 signals normalized to GAPDH are shown at the bottom. D) Intracellular calcium mobilization in leukocytes isolated from nonobese ($n = 3$) and obese ($n = 3$) individuals incubated with either vehicle, N-formylmethionyl-leucyl-phenylalanine (100 nM), or zymosan A (100 ng/ml) for 1 h at $37^{\circ}\text{C}/5\% \text{CO}_2$. fMLP, N-formylmethionyl-leucyl-phenylalanine; Non-Ob, nonobese; Ob, obese; Zym A, zymosan A. Results are means \pm SEM from 3 independent experiments assayed in quadruplicate.

cardiovascular disease as well as NAFLD, a condition that represents the hepatic manifestation of the metabolic syndrome (21). Considering the growing number of individuals affected by the current epidemic of obesity, especially the number of overweight children, the implementation of novel targeted strategies for the prevention of obesity-associated comorbidities is a matter of major interest. In this context, and considering that current anti-inflammatory therapies (*i.e.*, nonsteroidal anti-inflammatory and biologic drugs) are not an option for these patients because of their potential side effects, boosting the resolution of inflammation through increasing the formation of endogenous proresolving mediators is a well-positioned strategy to curbe the risks associated with obesity-induced inflammation. The current study provides relevant data in relation with this potential therapy. First, our findings confirm the inability of the immune systems of obese individuals to efficiently resolve the unremitting systemic inflammation that

persists in this condition. Second, our results provide evidence of an unbalanced situation in leukocytes from obese individuals between the enhanced formation of lipid mediators with proinflammatory properties and the formation of lipid mediators with proresolving activity (*e.g.*, SPMs). Third, our study provides novel mechanistic insights on the impaired formation of SPMs in leukocytes from obese individuals. Finally, our data provide proof of concept that intermediate precursors of SPM biosynthesis (*i.e.*, 17-HDHA and 18-HEPE) have the ability to override the impaired formation of these proresolving lipid mediators by obese leukocytes.

Previous studies from our laboratory and others have provided evidence of a heightened proinflammatory phenotype along with a compromised capacity to produce SPMs in white adipose tissue from obese individuals and from experimental models of obesity, including high-fat diet-induced obese, *ob/ob* obese, and *db/db* obese and diabetic mice (22–25). In the current study, we have



AQ:24 **Figure 6.** A) Schematic diagram of the biosynthesis of D-series Rvs through the actions of 15- and 5-LOX. B) Levels of D-series Rvs (RvD1, -2, -3, -4, -5, and -6) in leukocytes isolated (3×10^6 cells/condition) from healthy donors incubated with either vehicle (0.3% ethanol), 17-HDHA (1 μ M), or DHA (1 μ M) in the presence of zymosan A (100 ng/ml) for 30 min at 37°C/5% CO₂. C) Levels of D-series Rvs in leukocytes isolated from nonobese ($n = 5$) and obese ($n = 6$) individuals incubated with vehicle, 17-HDHA, or DHA in the presence of zymosan A for 30 min at 37°C/5% CO₂. Calculation of DHA-derived SPM:DHA and DHA-derived SPM:17-HDHA ratios in leukocytes from nonobese and obese subjects is shown as an inset. D) Ratios of D-series Rv:PG and D-series Rv:LTB₄ in leukocytes from nonobese and obese individuals. Non-Ob, nonobese; Ob, obese; Veh, vehicle. Results are means \pm SEM from 6 independent experiments assayed in duplicate. * $P < 0.05$, ** $P < 0.01$, *** $P < 0.001$ vs. vehicle or nonobese group.

B/W

expanded this concept of unbalanced SPM formation in obese white adipose tissue to the systemic circulation. Indeed, a major novelty of our study was the demonstration that the existing imbalance between enhanced formation of proinflammatory lipid mediators compared with that of SPMs also takes place in peripheral blood leukocytes isolated from individuals with morbid obesity. This observation has a major implication because it suggests that unresolved and unremitting inflammation is a generalized and common event in obesity. Moreover, our *in vitro* findings in leukocyte incubations suggest that unresolved inflammation in obesity is the result of impaired leukocyte SPM biosynthesis rather than increased loss of SPMs secondary to accelerated SPM inactivation (23).

Biosynthesis of the SPMs of the Rv D family is a complex process that involves the engagement of 15- and 5-LOX enzymes (6). In particular, the formation of D-series Rvs requires the initial conversion by 15-LOX of the omega-3 parent precursor DHA into 17-HDHA and the subsequent transformation by 5-LOX of this intermediate into 6 different molecular entities, namely RvD1, -2, -3, -4, -5, and -6 (26, 27). Indeed, the endogenous production of 17-HDHA was significantly reduced in leukocytes from obese individuals, an impairment that was also observed when these leukocytes were incubated with exogenous concentrations of DHA. This finding could be caused by a reduced uptake of DHA because in obese leukocytes, we found a remarkable decrease in the protein levels of the membrane transporter MFSD2A required for the cellular incorporation of DHA (16, 28). However, the observation that only 17-HDHA (derived from DHA through the activity of 15-LOX) was significantly reduced in obese leukocytes in the absence of changes in other monohydroxy fatty acids ~~enzymatically (14-HDHA by 12-LOX) or nonenzymatically (13-HDHA, 7-HDHA, and 4-HDHA)~~ derived from DHA suggests compromised 15-LOX activity in this condition. This is a potential mechanism that needs to be further explored, despite the fact that the expression of the 15-LOX isoenzymes was not reduced in obese leukocytes. In addition to this, our data demonstrated that 5-LOX protein levels and phosphorylation of Ser271 of 5-LOX were significantly reduced in leukocytes from obese individuals. Because Ser271 phosphorylation has been shown to inhibit the nuclear export of 5-LOX (29), these findings suggest that in obese leukocytes, 5-LOX would be mostly localized in the ~~cytoplasm~~ nucleus, which is a trait that would favor and not hamper the biosynthesis of SPMs by these cells (30–33). However, confocal microscopy analyses could not confirm this counterintuitive finding and only proved a less intense 5-LOX signal and a distinct intracellular redistribution of this enzyme in leukocytes from obese individuals. This finding, together with the absence of changes in the intracellular calcium mobilization and phosphorylation of upstream kinases implicated in the regulation of 5-LOX activity, supports the concept that impaired SPM production by obese leukocytes cannot simply be attributed to a dysfunctional 5-LOX pathway. This view is supported by the finding that the amount of D-series Rvs produced by obese leukocytes was similar to that of healthy leukocytes when they were incubated with exogenous 17-HDHA,

which is dependent on 5-LOX to convert into D-series Rvs. Collectively, these data suggest that unbalanced formation of Rvs of the D series with respect to proinflammatory lipid mediators such as LTB₄ in obese leukocytes could be the consequence of reduced 15-LOX activity together with a defective 5-LOX distribution.

In summary, our study provides data indicating that obese individuals produce an unbalanced amount of the proresolving lipid mediators derived from DHA (*i.e.*, Rvs of the D series) in peripheral leukocytes, and this is accompanied by an enhanced formation of lipid mediators with proinflammatory properties. The impaired formation of these DHA-derived SPMs is likely the consequence of an alteration in LOX activity, expression, or subcellular localization, leading to an altered 15-LOX/5-LOX sequential biosynthesis of SPMs. Notably, impaired formation of DHA-derived SPMs can be rescued by supplementation with the intermediate precursor 17-HDHA. These findings open new avenues for alternative approaches to the use of omega-3 fatty acids as a nutrition therapy to boost SPM formation to promote the resolution of inflammation. For instance, supplementation with the intermediate (*i.e.*, 17-HDHA) instead of the parent precursor (*i.e.*, DHA) could be of major significance in overcoming impaired SPM formation in conditions in which DHA metabolism is compromised, such as in the case of obesity. AQ:17

ACKNOWLEDGMENTS

The authors thank Anabel Martínez-Puchol for her technical assistance. This study was supported by the Spanish Ministerio de Educación y Ciencia (MEC) (SAF15/63674-R and PIE14/00045) under the European Regional Development Fund (ERDF). CIBERehd is funded by the Instituto de Salud Carlos III. Our laboratory is a Consolidated Research Group recognized by the Generalitat de Catalunya (2017SGR1449). This study was carried out at the Center Esther Koplowitz, IDIBAPS, which is part of the Centres de Recerca de Catalunya (CERCA) Programme and Generalitat de Catalunya. The authors declare no conflicts of interest. AQ:18
AQ:19

AUTHOR CONTRIBUTIONS

C. López-Vicario and J. Clària conceived and designed the experiments; C. López-Vicario performed the experiments; N. Pérez-Romero and M. Forné supervised clinical procedures; J. Dalli performed liquid chromatography–tandem mass spectrometry analysis; E. Titos, J. Alcaraz-Quiles, M. Casulleras, M. Durán-Güell, and R. Flores-Costa contributed reagents and tools and provided assistance to experiments; and C. López-Vicario and J. Clària wrote the manuscript. AQ:20

REFERENCES

1. Ferrante, A. W., Jr. (2007) Obesity-induced inflammation: a metabolic dialogue in the language of inflammation. *J. Intern. Med.* **262**, 408–414
2. Hotamisligil, G. S. (2006) Inflammation and metabolic disorders. *Nature* **444**, 860–867

3. Ouchi, N., Parker, J. L., Lugus, J. J., and Walsh, K. (2011) Adipokines in inflammation and metabolic disease. *Nat. Rev. Immunol.* **11**, 85–97
4. Unamuno, X., Gómez-Ambrosi, J., Rodríguez, A., Becerril, S., Frühbeck, G., and Catalán, V. (2018) Adipokine dysregulation and adipose tissue inflammation in human obesity. *Eur. J. Clin. Invest.* **48**, e12997
5. Lumeng, C. N., and Saltiel, A. R. (2011) Inflammatory links between obesity and metabolic disease. *J. Clin. Invest.* **121**, 2111–2117
6. Serhan, C. N. (2014) Pro-resolving lipid mediators are leads for resolution physiology. *Nature* **510**, 92–101
7. Spite, M., Clària, J., and Serhan, C. N. (2014) Resolvins, specialized proresolving lipid mediators, and their potential roles in metabolic diseases. *Cell Metab.* **19**, 21–36
8. Hellmann, J., Tang, Y., Kosuri, M., Bhatnagar, A., and Spite, M. (2011) Resolvin D1 decreases adipose tissue macrophage accumulation and improves insulin sensitivity in obese-diabetic mice. *FASEB J.* **25**, 2399–2407
9. González-Pérez, A., Horrillo, R., Ferré, N., Gronert, K., Dong, B., Morán-Salvador, E., Titos, E., Martínez-Clemente, M., López-Parra, M., Arroyo, V., and Clària, J. (2009) Obesity-induced insulin resistance and hepatic steatosis are alleviated by omega-3 fatty acids: a role for resolvins and protectins. *FASEB J.* **23**, 1946–1957
10. Titos, E., Rius, B., González-Pérez, A., López-Vicario, C., Morán-Salvador, E., Martínez-Clemente, M., Arroyo, V., and Clària, J. (2011) Resolvin D1 and its precursor docosahexaenoic acid promote resolution of adipose tissue inflammation by eliciting macrophage polarization toward an M2-like phenotype. *J. Immunol.* **187**, 5408–5418
11. Rius, B., Titos, E., Morán-Salvador, E., López-Vicario, C., García-Alonso, V., González-Pérez, A., Arroyo, V., and Clària, J. (2014) Resolvin D1 primes the resolution process initiated by calorie restriction in obesity-induced steatohepatitis. *FASEB J.* **28**, 836–848
12. Neuhofer, A., Zeyda, M., Mascher, D., Itariu, B. K., Murano, I., Leitner, L., Hochbrugger, E. E., Fraisl, P., Cinti, S., Serhan, C. N., and Stulnig, T. M. (2013) Impaired local production of proresolving lipid mediators in obesity and 17-HDHA as a potential treatment for obesity-associated inflammation. *Diabetes* **62**, 1945–1956
13. Chatterjee, A., Komshian, S., Sansbury, B. E., Wu, B., Mottola, G., Chen, M., Spite, M., and Conte, M. S. (2017) Biosynthesis of proresolving lipid mediators by vascular cells and tissues. *FASEB J.* **31**, 3393–3402
14. Dalli, J., Colas, R. A., and Serhan, C. N. (2013) Novel n-3 immunoresolvents: structures and actions. *Sci. Rep.* **3**, 1940; erratum: 4, 6726
15. Rathod, K. S., Kapil, V., Velmurugan, S., Khambata, R. S., Siddique, U., Khan, S., Van Eijl, S., Gee, L. C., Bansal, J., Pitrola, K., Shaw, C., D'Acquisto, F., Colas, R. A., Marelli-Berg, F., Dalli, J., and Ahluwalia, A. (2017) Accelerated resolution of inflammation underlies sex differences in inflammatory responses in humans. *J. Clin. Invest.* **127**, 169–182
16. Nguyen, L. N., Ma, D., Shui, G., Wong, P., Cazenave-Gassiot, A., Zhang, X., Wenk, M. R., Goh, E. L., and Silver, D. L. (2014) Mfsd2a is a transporter for the essential omega-3 fatty acid docosahexaenoic acid. *Nature* **509**, 503–506
17. Rådmark, O., Werz, O., Steinhilber, D., and Samuelsson, B. (2007) 5-Lipoxygenase: regulation of expression and enzyme activity. *Trends Biochem. Sci.* **32**, 332–341
18. Luo, M., Jones, S. M., Peters-Golden, M., and Brock, T. G. (2003) Nuclear localization of 5-lipoxygenase as a determinant of leukotriene B4 synthetic capacity. *Proc. Natl. Acad. Sci. USA* **100**, 12165–12170
19. Werz, O., Szellas, D., Steinhilber, D., and Rådmark, O. (2002) Arachidonic acid promotes phosphorylation of 5-lipoxygenase at Ser-271 by MAPK-activated protein kinase 2 (MK2). *J. Biol. Chem.* **277**, 14793–14800
20. Capodici, C., Pillinger, M. H., Han, G., Philips, M. R., and Weissmann, G. (1998) Integrin-dependent homotypic adhesion of neutrophils. Arachidonic acid activates Raf-1/Mek/Erk via a 5-lipoxygenase-dependent pathway. *J. Clin. Invest.* **102**, 165–175
21. Abdelaal, M., le Roux, C. W., and Docherty, N. G. (2017) Morbidity and mortality associated with obesity. *Ann. Transl. Med.* **5**, 161
22. Titos, E., Rius, B., López-Vicario, C., Alcaraz-Quiles, J., García-Alonso, V., Lopategi, A., Dalli, J., Lozano, J. J., Arroyo, V., Delgado, S., Serhan, C. N., and Clària, J. (2016) Signaling and immunoresolving actions of resolvin D1 in inflamed human visceral adipose tissue. *J. Immunol.* **197**, 3360–3370
23. Clària, J., Dalli, J., Yacoubian, S., Gao, F., and Serhan, C. N. (2012) Resolvin D1 and resolvin D2 govern local inflammatory tone in obese fat. *J. Immunol.* **189**, 2597–2605
24. Clària, J., Nguyen, B. T., Madenci, A. L., Ozaki, C. K., and Serhan, C. N. (2013) Diversity of lipid mediators in human adipose tissue depots. *Am. J. Physiol. Cell Physiol.* **304**, C1141–C1149
25. White, P. J., Arita, M., Taguchi, R., Kang, J. X., and Marette, A. (2010) Transgenic restoration of long-chain n-3 fatty acids in insulin target tissues improves resolution capacity and alleviates obesity-linked inflammation and insulin resistance in high-fat-fed mice. *Diabetes* **59**, 3066–3073
26. Serhan, C. N., Clish, C. B., Brannon, J., Colgan, S. P., Chiang, N., and Gronert, K. (2000) Novel functional sets of lipid-derived mediators with antiinflammatory actions generated from omega-3 fatty acids via cyclooxygenase 2-nonsteroidal antiinflammatory drugs and transcellular processing. *J. Exp. Med.* **192**, 1197–1204
27. Hong, S., Lu, Y., Yang, R., Gotlinger, K. H., Petasis, N. A., and Serhan, C. N. (2007) Resolvin D1, protectin D1, and related docosahexaenoic acid-derived products: analysis via electrospray/low energy tandem mass spectrometry based on spectra and fragmentation mechanisms. *J. Am. Soc. Mass Spectrom.* **18**, 128–144
28. Ungaro, F., Tacconi, C., Massimino, L., Corsetto, P. A., Correale, C., Fonteyne, P., Piontini, A., Garzarella, V., Calcaterra, F., Della Bella, S., Spinelli, A., Carvello, M., Rizzo, A. M., Vetrano, S., Petti, L., Fiorino, G., Furfaro, F., Mavilio, D., Maddipati, K. R., Malesci, A., Peyrin-Biroulet, L., D'Alessio, S., and Danese, S. (2017) MFSD2A promotes endothelial generation of inflammation-resolving lipid mediators and reduces colitis in mice. *Gastroenterology* **153**, 1363–1377.e6
29. Flamand, N., Luo, M., Peters-Golden, M., and Brock, T. G. (2009) Phosphorylation of serine 271 on 5-lipoxygenase and its role in nuclear export. *J. Biol. Chem.* **284**, 306–313
30. Rouzer, C. A., and Samuelsson, B. (1987) Reversible, calcium-dependent membrane association of human leukocyte 5-lipoxygenase. *Proc. Natl. Acad. Sci. USA* **84**, 7393–7397
31. Coffey, M., Peters-Golden, M., Fantone, J. C. III, and Sporn, P. H. (1992) Membrane association of active 5-lipoxygenase in resting cells. Evidence for novel regulation of the enzyme in the rat alveolar macrophage. *J. Biol. Chem.* **267**, 570–576
32. Fredman, G., Ozcan, L., Spolitu, S., Hellmann, J., Spite, M., Backs, J., and Tabas, I. (2014) Resolvin D1 limits 5-lipoxygenase nuclear localization and leukotriene B4 synthesis by inhibiting a calcium-activated kinase pathway. *Proc. Natl. Acad. Sci. USA* **111**, 14530–14535
33. Werz, O., Gerstmeier, J., Libreros, S., De la Rosa, X., Werner, M., Norris, P. C., Chiang, N., and Serhan, C. N. (2018) Human macrophages differentially produce specific resolvin or leukotriene signals that depend on bacterial pathogenicity. *Nat. Commun.* **9**, 59

Received for publication November 30, 2018.
Accepted for publication February 11, 2019.